Importance of charging in atomic resolution scanning tunneling microscopy: Study of a single phosphorus atom in a Si(001) surface

M. W. Radny,[1] P. V. Smith,[1] T. C. G. Reusch,[2] O. Warschkow,[3] N. A. Marks,[3] H. F. Wilson,[3] N. J. Curson,[2] S. R. Schofield,[1] D. R. McKenzie,[3] and M. Y. Simmons[2]

[1]*School of Mathematical and Physical Sciences, The University of Newcastle, Callaghan 2308, Australia*

[2]*Centre for Quantum Computer Technology, School of Physics, The University of New South Wales, Sydney 2052, Australia*

[3]*Centre for Quantum Computer Technology, School of Physics, The University of Sydney, Sydney 2006, Australia*

(Received 3 July 2006; published 27 September 2006)

We present a detailed voltage-dependent scanning tunneling microscopy study of a single phosphorus atom in the Si(001) surface. Using density functional theory calculations we show that tip-induced charging results in reversible structural and electronic changes. These changes are caused by charge transfer from delocalized surface states to localized states associated with the presence of the phosphorus atom. While two stable geometric configurations are predicted, only the higher energy configuration is consistent with experiment.

DOI: 10.1103/PhysRevB.74.113311 PACS number(s): 68.35.Bs, 68.37.Ef, 68.43.−h, 73.20.−r

Scanning tunneling microscopy (STM) is a widely used technique for the identification of atomic-scale defects and adsorbates on semiconductor surfaces. The assignment of the geometric and electronic structure is commonly achieved by a comparison of high-resolution experimental STM data with first-principles calculations and simulated STM images.[1] However, in recent years experimental and theoretical evidence has been accumulating that STM is an invasive probe which can induce structural changes to species on the surface.[2,3] While this has been used intentionally to modify surface species such as hydrogen, chlorine, and biphenyl on Si(001),[2] it has also been observed as an unavoidable side effect when imaging ethylene, antimony, and potassium.[3]

In this paper, we report the results of a combined theoretical and experimental STM study of a single phosphorus atom in the Si(001) surface. The appearance of the P-induced feature in STM imaging displays a complex dependence on the bias voltage. To understand this behavior we have undertaken a detailed theoretical investigation using spin-polarized density functional theory calculations in which we specifically include the effect of a tip-induced shift in the Fermi energy (E_F) and charging of the surface feature. We demonstrate that the STM induces reversible geometric and electronic changes even under standard imaging conditions. These changes arise from charge transfer between delocalized and localized surface states near the Fermi level associated with the embedded P atom. Surprisingly, it is the electronic structure of the second lowest geometric configuration (and not the ground state) that consistently explains the appearance and bias dependence of the experimental STM images.

When phosphorus is incorporated into the Si(001) surface it forms a Si-P heterodimer.[4,5] Due to the higher valence of phosphorus the one additional (unpaired) electron relative to the Si-Si dimer [Fig. 1(a)] has long been considered as occupying the dangling bond orbital of the heterodimer Si atom[4] [Fig. 1(b)]. This interpretation is based on STM observations showing a bright protrusion on the same dimer end of the heterodimer for both filled and empty states.[4,5] Ab initio periodic slab calculations for Si-As heterodimers (valence-isoelectronic with Si-P) using a small (2×2) surface unit cell also showed a high density of states on the same dimer end for filled and empty states,[6] lending support to the picture of a half-occupied dangling bond orbital. Our bias-dependent STM studies and ab initio calculations show, however, that this picture is inaccurate and that the additional electron associated with the phosphorus atom is in fact delocalized over the surface, resulting in a locally charged heterodimer [Fig. 1(c)] isoelectronic to a Si-Si dimer [Fig. 1(a)]. Moreover, we will show that in bias-dependent imaging, STM-induced charge accumulation[7] can lead to occupation of the heterodimer Si atom dangling bond orbital, which results in an inversion of the buckling angle of the heterodimer.

In Figs. 2(a)–2(f), we show detailed bias-dependent STM images taken at room temperature of an isolated Si-P heterodimer on an n-type Si(001) substrate.[8] The high-bias filled-state appearance in Fig. 2(c) matches previous reports[5,6] where a bright protrusion is seen on one dimer end, and the heterodimer induces static buckling of the neighboring Si-Si dimers. However, in our STM experiments, we find that this protrusion darkens continuously [Figs. 2(a) and 2(b)] as the filled-state imaging bias is reduced, which cannot be explained by a singly occupied dangling bond. In empty-state images [Figs. 2(d)–2(f)], the bright protrusion can be seen at all biases. At high empty-state bias [Figs. 2(e) and 2(f)], these images also show a pronounced halo extending over 2–3 nm, which indicates positive charging.[7] Similar bias-dependent changes in Si-P appearance have been observed by us using different tips and samples and are fully reversible.

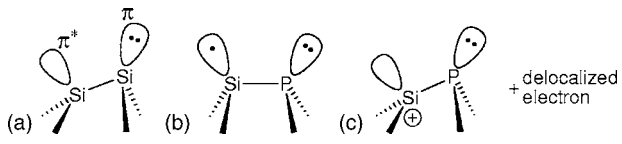

FIG. 1. Schematic representations of (a) a buckled Si-Si dimer on the Si(001) surface with one doubly occupied and one empty dangling bond, giving rise to occupied π and unoccupied π^* surface bands, (b) the near-planar, dangling bond model of the Si-P heterodimer,[5,7] and (c) the locally charged, ground state heterodimer structure proposed in this work.

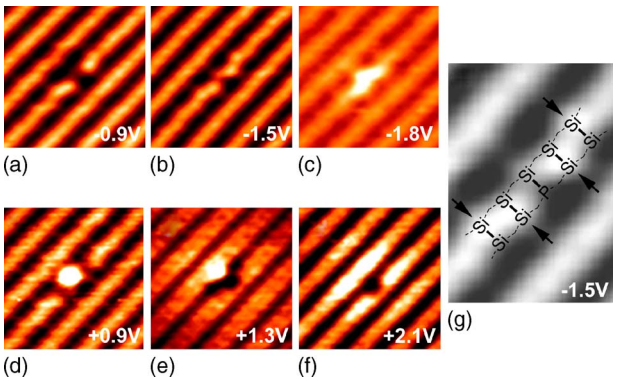

FIG. 2. (Color online) Bias-dependent filled-state (a)–(c) and empty-state (d)–(f) STM images for a Si-P heterodimer on a low-dosed annealed Si(001) surface. Panel (g) shows a magnified view of panel (b) and the orientation of the heterodimer in these images (see text). Up-buckled Si atoms are indicated by black arrows, showing the heterodimer to be in the HD1 configuration (cf. Fig. 3).

To account for the observed STM appearance of the Si-P heterodimer, we have conducted spin-polarized density functional calculations using a slab model of the Si(001) surface in which a single heterodimer is embedded. The calculations were carried out using the VASP code,[9] ultrasoft pseudopotentials,[10] a 173.5 eV planewave cutoff, and the generalized gradient approximation (PW91).[11] The slab model consisted of up to six Si layers plus a terminating dihydride layer and a vacuum of ~10 Å. Calculations were performed using (2×4), (2×6), (4×4), and (6×6) surface unit cells with the irreducible surface Brillouin zones sampled by four special k points.

For all unit cell sizes, two stable configurations for the Si-P heterodimer were predicted by our calculations. These are illustrated schematically in Fig. 3. In configuration HD2 [Fig. 3, top row], the adjacent Si-Si dimers are buckled such that the Si atoms next to the P atom of the heterodimer are buckled downward. In configuration HD1 [Fig. 3, bottom row], the Si-Si dimers are buckled in the opposite sense; that is, the Si atoms of the dimers next to the P atom are buckled upward. In all our calculations the values of the buckling

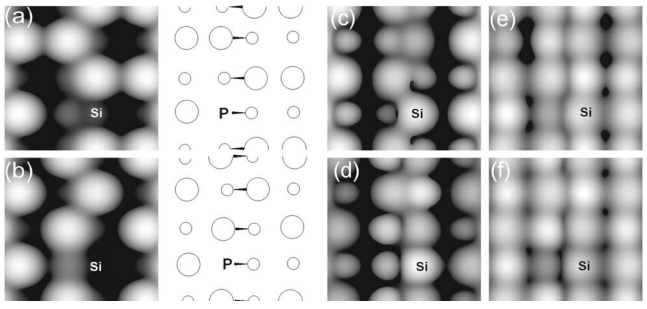

FIG. 3. Atomic structures and simulated filled-state (a) and (b) and empty-state (c)–(f) STM images for the HD1 (bottom row) and HD2 (top row) configurations. Large and small circles in the structure diagrams denote up and down Si atoms, respectively. Note how the HD1 configuration breaks the alternating sequence of up- and down-buckled dimers on the Si(001) surface. The simulated images are for an isosurface value of 2.5×10^{-4} e/Å^3.

TABLE I. Calculated Si-P heterodimer buckling angle (in degrees) and bond length (in angstroms, given in parentheses) as a function of surface unit cell size for configurations HD1 and HD2.

	(2×4)	(2×6)	(4×4)	(6×6)
HD1	5.6 (2.32)	9.3 (2.29)	14.6 (2.26)	15.1 (2.26)
HD2	15.6 (2.30)	15.3 (2.30)	15.5 (2.30)	15.3 (2.31)

angles/bond lengths of the Si-Si dimers adjacent to the heterodimer of ~19°/2.4 Å were found to be similar to those on the clean surface. Any significant geometrical changes that result from the presence of the P atom in the surface are limited to the Si-P heterodimer itself.

In Table I we summarize the calculated geometrical parameters of the heterodimer in the HD1 and HD2 configurations as a function of surface unit cell size. The buckling angle predicted for the Si-P heterodimer in HD1 shows a sharp increase from ~6° to ~15° with increasing cell size, with the Si atom being the down atom. In contrast, the buckling angle for HD2 is around 15° for all unit cell sizes considered. We see that in the limit of large cell size both the HD1 and HD2 configurations adopt a strongly buckled geometry, similar to that of a Si-Si dimer. As we will show below, this similarity in geometry arises because the unpaired electron is not present at the heterodimer Si atom site as previously believed[4] but is, in fact, delocalized. This renders the heterodimer locally cationic [Fig. 1(c)], and thus isoelectronic and isostructural to a Si-Si dimer [Fig. 1(a)].

The dark appearance of the heterodimer in the low-bias filled-state STM images [Fig. 2(a)] indicates that the unpaired electron is delocalized on the surface. This is evident in Fig. 3, which shows the calculated local density of states for the (4×4) cell integrated over −1.0 eV (a, b), +0.6 eV (c, d), and +1.0 eV (e, f), from the Fermi level. These plots reveal the spatial distribution of the surface energy bands relevant to imaging[12] and can be compared directly with the experimentally observed STM images. In the filled-state plots [Figs. 3(a) and 3(b)], the brightest features are those associated with the up-buckled atoms of the Si-Si dimers. In both configurations, the heterodimer Si atom appears quite dark, showing that the unpaired electron is not present in the dangling bond orbital at this site. The simulated empty-state images [Figs. 3(c)–3(f)] show that the heterodimer Si atom images more brightly than the P atom. This determines the orientation of the heterodimer in the experimental images. Comparing the buckling sequence of the simulated and experimental filled-state images [Figs. 3(a) and 3(b), and Figs. 2(a) and 2(g)] establishes unambiguously that it is the HD1 configuration that is observed. The delocalization of the unpaired electron highlights that the isolated dangling bond of the heterodimer must be treated as an extended defect. This provides an explanation for the shortcomings of earlier theoretical models of the heterodimer,[4,6] where slab and clusters were too small to adequately account for the delocalization of the unpaired electron.

While delocalization of the unpaired electron accounts for the dark appearance of the Si-P heterodimer at low filled-state bias [Fig. 2(a)], it is the sensitivity of the HD1 het-

TABLE II. Heterodimer buckling angles (in degrees) and bondlengths (in angstroms, given in parentheses) calculated for HD1 and HD2 with zero, one, and two additional electrons in the (4×4) surface unit cell.

	N_e	N_e+1	N_e+2
HD1	14.6 (2.26)	3.2 (2.33)	−5.7 (2.42)
HD2	15.5 (2.30)	15.7 (2.30)	15.8 (2.29)

erodimer buckling angle on surface cell size (Table I) that provides an important clue in explaining the transition to a brightly imaging heterodimer at higher filled-state bias [Fig. 2(c)]. A decrease in the cell size increases the density of additional (unpaired) electrons on the surface (due to the higher heterodimer coverage) and leads to the charging of the Si site of the heterodimer evident in the reduction of its buckling angle. By analogy, we might expect that a shift in E_F due to STM tip-induced band bending[7] on the n-type substrate would also lead to a localization of charge on the heterodimer.

In order to confirm this charge localization effect, we have carried out further calculations for HD1 and HD2 with one and two additional electrons in a (4×4) unit cell. We denote these systems as (N_e+1) and (N_e+2), where N_e is the number of electrons in the neutral cell. In our calculations, this additional charge has been compensated by a uniform background. The calculated buckling angle and bond length values are presented in Table II. The HD2 configuration is seen to remain unaffected by the addition of electrons, while the HD1 configuration changes from a downward buckled $(\sim15°)$ heterodimer in the (N_e) case, to a near planar heterodimer $(\sim3°)$ in the (N_e+1) case, and to an upwards buckling of the heterodimer Si atom $(\sim-6°)$ for the (N_e+2) case. The heterodimer bond length also increases from 2.26 Å (N_e) to 2.42 Å (N_e+2). Since changes in the Si-P heterodimer buckling angle indicate charging of the heterodimer Si atom (Table I), we see that the addition of electrons leads to charge localization for the HD1 configuration, but not for HD2.

The localization of additional charge for HD1 is clearly revealed in the series of simulated filled-state STM images shown in Fig. 4. With the addition of electrons to the system, the heterodimer Si site is seen to brighten from a dark feature

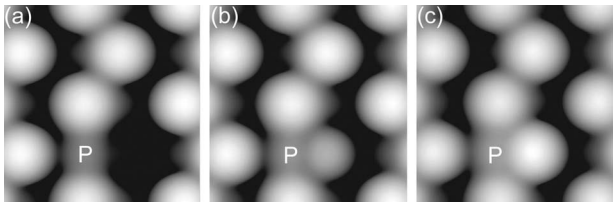

FIG. 4. Simulated filled-state STM images for a HD1 heterodimer in a (4×4) unit cell: (a) (N_e), (b) (N_e+1), and (c) (N_e+2). Each image is for an isosurface value of 2.5×10^{-4} e/Å^3. Of the one and two additional electrons in the (N_e+1), and (N_e+2) calculations, 0.6 and 1.4 electrons, respectively, are located within a sphere of radius 3.0 Å around the heterodimer silicon atom.

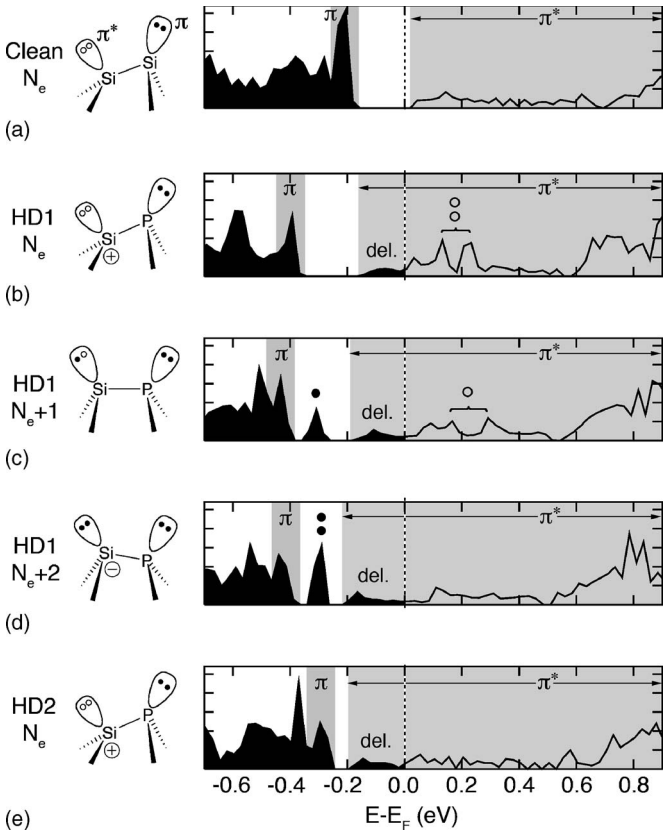

FIG. 5. The electronic DOS in the vicinity of the Fermi level (vertical dashed line) for (a) a neutral clean surface, and (b) (N_e) HD1, (c) (N_e+1) HD1, (d) (N_e+2) HD1, and (e) (N_e) HD2 configurations. Occupied states are filled in black, and the gray background indicates the range of the π- and π^* surface bands. The filled and empty circles indicate the localized HD1 defect state and its occupancy. The population of π^* by the delocalized unpaired electron [(b) and (e)] and the delocalized charge due to STM-induced band bending [(c) and (d)] is also indicated.

in Fig. 4(a) to a very bright appearance in Fig. 4(c). This behavior is in excellent agreement with the experimental data [Figs. 2(a)–2(c)]. The progressive brightening of the heterodimer with increasing filled-state bias is thus understood to be due to an STM-induced shift in E_F. This causes an accumulation of electronic charge and its localization on the heterodimer Si atom, together with an upward relaxation of this atom.

Insight into why only the HD1 configuration is sensitive to the addition of electrons is provided by the electronic densities of states (DOS) plotted in Fig. 5. In comparison with the clean Si(001) surface [Fig. 5(a)], the DOS for the (N_e) HD1 configuration [Fig. 5(b)] shows delocalization of the unpaired electron over the lower part of the π^* band as well as a pronounced defect level in this band (split into two due to interaction with the π^* band[13]). This defect level represents the unoccupied heterodimer Si atom dangling bond orbital. It is the appearance of this level near E_F that causes the susceptibility of the HD1 configuration to structural and electronic changes. These changes are activated by tip-induced band bending in the surface and are illustrated in Figs. 5(b)–5(d). We observe that increasing the electron den-

sity moves this defect level below E_F into the gap between the π and π^* bands, completely decoupling it from the bulk and surface bands. Occupation of this defect level gives rise to charge localization on the Si heterodimer dangling bond. This results in the observed local charging of the heterodimer and the associated changes in its buckling geometry. It is thus the behavior of the localized defect level near E_F for the HD1 configuration that leads to the bias-dependent features in the experimental and theoretically simulated STM data shown in Figs. 2(a)–2(c) and Figs. 4(a)–4(c), respectively.

By contrast, the HD2 configuration cannot explain the observed bias dependence. This is because a similar localized defect level does not occur near E_F for the HD2 configuration [Fig. 5(e)] and hence, any additional electrons in HD2 will simply progressively occupy the low-energy, dispersive π^* surface states. The additional electrons are thus always delocalized over the surface, preserving its atomic and electronic structure (cf. Table II). It is interesting to note, however, that our calculations predict the HD2 (N_e) configuration (with its alternating buckling geometry) to be 0.13 eV more stable than the symmetry-breaking HD1. This energy difference mirrors the alternating buckling preference of a Si-Si dimer on the bare surface (0.12 eV). While STM images of the clean Si(001) surface show that alternate buckling is preferred, the equivalent HD2 configuration is clearly not the observed structure for the Si-P heterodimer system. It remains an ongoing question why the energetically disfavored and counterintuitive HD1 configuration, rather than the HD2 configuration, is observed in the STM experiments.

In summary, we have demonstrated the importance of STM-induced charging for the identification of atomic-scale features in the silicon surface. Detailed bias-dependent STM imaging in combination with density functional theory band structure calculations has shown that reversible charge transfer between delocalized and localized states causes changes in both the geometric and electronic structure of a Si-P heterodimer in the Si(001) surface. Similar behavior is anticipated for other defects and adsorbates on semiconductor surfaces that give rise to localized surface states close to the Fermi level.

ACKNOWLEDGMENTS

This work was supported by the Australian Research Council, the Australian Partnership for Advanced Computing, the Australian Government, the Semiconductor Research Corporation, the U.S. Advanced Research and Development Activity, and the National Security Agency and Army Research Office under contract DAAD19-01-1-0653.

[1] G. A. D. Briggs and A. J. Fisher, Surf. Sci. Rep. **33**, 1 (1999); W. A. Hofer, Prog. Surf. Sci. **71**, 147 (2003).

[2] U. J. Quaade, K. Stokbro, C. Thirstrup, and F. Grey, Surf. Sci. **415**, L1037 (1998); J. J. Boland, Science **262**, 1703 (1993); Y. Nakamura, Y. Mera, and K. Maeda, Surf. Sci. **531**, 68 (2003); M. Lastapis, M. Martin, D. Riedel, L. Hellner, G. Comtet, and G. Dujardin, Science **308**, 1000 (2005).

[3] H. Ness and A. J. Fisher, Phys. Rev. B **55**, 10081 (1997); A. Pomyalov, Phys. Rev. B **57**, 8989 (1998).

[4] Y. Wang, X. Chen, and R. J. Hamers, Phys. Rev. B **50**, 4534 (1994); R. J. Hamers, Y. Wang, and J. Shan, Appl. Surf. Sci. **107**, 25 (1996).

[5] N. J. Curson, S. R. Schofield, M. Y. Simmons, L. Oberbeck, J. L. O'Brien, and R. G. Clark, Phys. Rev. B **69**, 195303 (2004).

[6] B. D. Yu and A. Oshiyama, Phys. Rev. Lett. **71**, 585 (1993).

[7] G. W. Brown, H. Grube, M. E. Hawley, S. R. Schofield, N. J. Curson, M. Y. Simmons, and R. G. Clark, J. Appl. Phys. **92**, 820 (2002).

[8] The surface was flash-annealed at 1100 °C, dosed with 0.001 L of PH_3, and annealed for 10 s at 550 °C.

[9] G. Kresse and J. Hafner, Phys. Rev. B **47**, 558 (1993); G. Kresse and J. Hafner, *ibid.* **49**, 14251 (1994); G. Kresse and J. Furthmüller, *ibid.* **54**, 11169 (1996).

[10] D. Vanderbilt, Phys. Rev. B **41**, 7892 (1990).

[11] J. P. Perdew, J. A. Chevary, S. H. Vosko, K. A. Jackson, M. R. Pederson, D. J. Singh, and C. Fiolhais, Phys. Rev. B **46**, 6671 (1992).

[12] J. Tersoff and D. R. Hamann, Phys. Rev. Lett. **50**, 1998 (1985).

[13] M. W. Radny, P. V. Smith, T. C. G. Reusch, O. Warschkow, N. A. Marks, H. F. Wilson, N. J. Curson, S. R. Schofield, D. R. McKenzie, and M. Y. Simmons (unpublished).